Thickness measurement of transparent plates by a self-mixing interferometer

Mohammad Taghi Fathi* and Silvano Donati
Dipartimento di Elettronica, Università degli Studi di Pavia, 27100 Pavia, Italy
**Corresponding author: mohammad.fathi@unipv.it*

Received March 3, 2010; revised April 22, 2010; accepted April 26, 2010;
posted April 30, 2010 (Doc. ID 124960); published May 24, 2010

We introduce a technique to measure transparent glass slab thickness. It employs a very simple setup combining two interferometers: a forward-going beam scheme and a self-mixing readout of the beam reflected back to the laser source. Interestingly, the difference of the two readouts provides a quantity related to thickness measurement, irrespective of refractive index. We demonstrate this method using samples on a range of thickness from 30 to 1000 μm.

OCIS codes: 120.0120, 120.3180.

Noncontact optical measurement of thickness and refractive index of glass and thin films are of importance in a number of applications, and many different methods have been proposed and demonstrated. In addition to classical methods based on refraction and reflection [1–3], several authors have proposed interferometric schemes [4–8]. These schemes yield a measurement of the optical path length nkd (and not separately d or n) so that, to obtain thickness d, we have to know n or need to combine two measurement methods to solve for both n and d. In this Letter, we present a simple method of measuring the thickness of glass and a thin film slab, irrespective of refractive index, using a self-mixing interferometer (SMI), an arrangement that can sense the phase of a backscattered beam [9–11].

As shown in Fig. 1, in an SMI, the collimated beam from a laser diode (LD) is passed through the sample, and upon reflection from a photodiode (PD2) entrance window, a small fraction of the optical field is allowed to reenter the LD cavity. Here, the weak signal interacts coherently with the preexisting field in a process described as self-mixing [9,10]. The result is a modulation (in amplitude and frequency, AM and FM) of the lasing field, the modulating drive being the optical path length nkL. The amplitude modulation of the emitted power is easily detected by a photodiode, for example, one mounted on the rear facet of the LD. From the photodiode output current we get an interferometric signal of the type $I_0 \cos 2nkL$ carrying the phase information related to the path length of light from the LD to PD2 and back. Now we can rotate the slab as indicated in Fig. 1 and look at the dependence of $2nkL$ from the angle α.

The interferometric signal $\cos 2nkL$ is detected by photodiode PD1, usually a power-monitor photodiode made available in the LD package. Thus, the SMI is a very straightforward single-channel configuration that does not require a reference arm and has a minimum optical part count.

Now let us consider the second photodiode, PD2, in the setup of Fig. 1. This photodiode has an optical entrance window that already provides a few percent reflection, i.e., a return to the LD that is more than adequate to get a sizeable self-mixing modulation [10]. Additionally, photodiode PD2 receives the direct beam and, partially superposed to it, the double-reflected beam that crosses the slab under measurement twice. Thus, we obtain at PD2, as a detected current, a so-called shear interferometer signal similar to that described in [4].

Thus, from our straightforward and self-aligned setup, we obtain a pair of simultaneous signal outputs from PD1 and PD2 that depend upon the slab angle α. From these

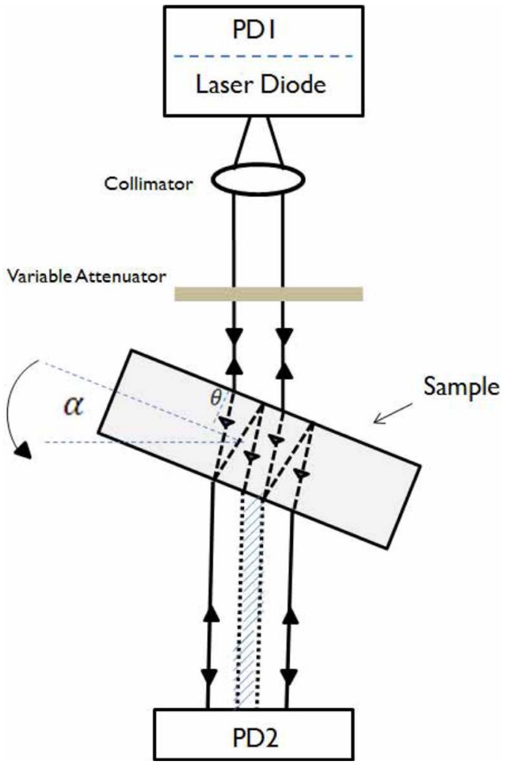

Fig. 1. (Color online) Experimental setup for thickness measurement with the SMI and self-reference interferometer method. The beam from a laser diode goes across the slab under measurement and reaches PD2; a few percent of power is also reflected by the photodiode entrance window. The back-reflected rays trace back the path and reenter the laser cavity, producing a SMI interferometric signal that carries the phase $2nkL$ as an amplitude modulation of the power at photodiode PD2. Another signal is provided by photodiode PD2, where we find the superposition (partial, with lateral shift) of transmitted and double-reflected beams in the slab (i.e., a shear interferometer). Upon rotation of the slab by an angle α, the two signals at PD1 and PD2 vary and provide signals to compute n and d.

signals, we are able to derive both n and d, as will be shown below.

Regarding the signal from the SMI, the power emitted by the LD is amplitude modulated by an interferometric waveform $F(\varphi)$, which is a periodic function with phase $\varphi = 2ks$, where $k = 2\pi/\lambda$ is the wavenumber, λ is wavelength in vacuum, and $s = L$ is the variation of distance from the LD to the PD2 entrance window. The power emitted by the LD can then be written as

$$P(\varphi) = P_0[1 + mF(\varphi)], \tag{1}$$

where P_0 is the power emitted by the unperturbed LD and m is a modulation index. The actual shape of the function $F(\varphi)$ depends on feedback parameter C, which, in turn, depends on laser parameters, target distance s, and the power reflectivity R_{eff} [10,11]. For our purpose, we decide to stay in the weak self-mixing regime ($C \ll 1$) so that, conveniently, $F(\varphi)$ is a cosine function. This is easily obtained by keeping low (a few percent) reflection from the PD2 entrance window. (An attenuator is used to decrease the back-injected signal as necessary.)

In propagating through the sample, the outgoing beam experiences two reflections at the air–sample interfaces, so there are two lateral sheared waves with different phases. Additional reflections are much smaller and can be neglected. Next to the sample, these waves are superimposed and produce an interference pattern. By rotation of the sample, this pattern is changed as the waves' superimposition sweeps from constructive to destructive interference and back. Analyzing the ray propagation, the phase difference between the transmitted beam and the double-reflected beam as seen by detector PD2 is a function of internal refraction θ that can be easily written as

$$\Delta\varphi_{\mathrm{PD}} = 2knd\cos\theta, \tag{2}$$

where n is the refractive index of the sample, d is the physical thickness of the sample, and θ is the angle (Fig. 1) of internal refraction.

Regarding the beam reflected back, after some lengthy but simple algebra, the phase-difference dependence from rotation angle α can be calculated as

$$\Delta\varphi_{\mathrm{SMI}} = 2kd(n\cos\theta - \cos\alpha). \tag{3}$$

In Eqs. (2) and (3), we find two unknowns, n and d. Favorably, by subtraction of Eq. (2) from Eq. (3) we get

$$\Delta\varphi = \Delta\varphi_{\mathrm{PD}} - \Delta\varphi_{\mathrm{SMI}} = 2kd\cos\alpha, \tag{4}$$

a result no more dependent upon n. Thus, by measuring the phase difference $\Delta\varphi$ at given rotation α, we can find d. Thereafter, we can also go back to Eq. (2) and solve for n, as well. As a good strategy for extracting the information contained in experimental data, we sweep α by a rotatory stage and look at the interferometric signal $\cos\Delta\varphi$ maxima and minima, whose difference is π rad between successive extrema, and equate π to the right-hand side of Eq. (2), $2kd(\cos\alpha_1 - \cos\alpha_2)$.

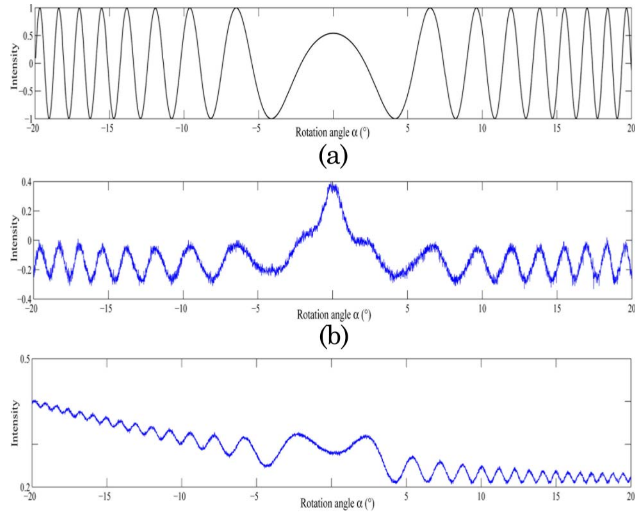

(a)

(b)

(c)

Fig. 2. (Color online) (a) Theoretical SMI phase variation; (b) experimental SMI signal; (c) experimental signal of forward-going interferometer. All results are plotted against rotation angle (degree) for a glass slab thickness of 154 μm.

To test the above concepts, we have used a diode laser as the source, a GaAlAs triple quantum-well semiconductor laser from Hitachi (HL8325G), emitting up to 20 mW at $\lambda = 832$ nm on a single longitudinal mode with good side-mode suppression (typically 30 dB). The diode laser was fed by a constant current supply and was TEC-controlled to avoid mode hopping. A collimating objective lens supplied by the manufacturer gives a nearly circular spot with a 2 mm diameter. Several glass slabs have been used as the sample, mounted upon a rotating dc motor running at constant speed, adjustable by constant voltage. The angular swing provided by the motorized rotating stage was about ±15°. The photodiodes were terminated on a high-Z transimpedance operational amplifier to ensure reasonable bandwidth and low noise. The signals from the photodetectors were, of course, of the type $I = I_0(1 + \cos\Delta\varphi)$, with $\Delta\varphi$ given either by Eq. (2) or Eq. (3). As an illustration, waveforms of detected signals of the SMI method, theoretical and experimental, as a function of rotation angle are shown in Figs. 2(a) and 2(b), respectively. In comparing the two curves, it is seen that the general trend of phase variation is matched. The peak artifact near-zero angle in the experiment is attributed to the reflection at the first slab surface. Experimental results of forward-going interferometry pattern are

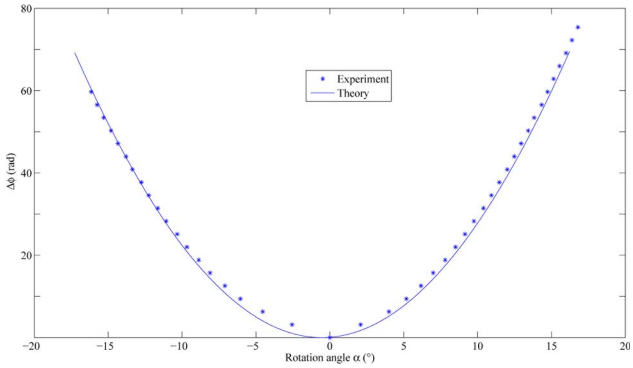

Fig. 3. (Color online) Experimental phase difference $\Delta\varphi_{\mathrm{PD}} - \Delta\varphi_{\mathrm{SMI}}$ for a 154 μm slab and the theoretical line providing the best least-square-fit interpolation.

Table 1. Thickness Experimental Results for Some Glass Samples

Measured Thickness (μm) Mechanical $\pm 2\%$	Measured Thickness (μm) Optical
29	27 ± 1
77	74 ± 2
154	157 ± 3
970	940 ± 15

shown in Fig. 2(c), the term to be subtracted ($\Delta\varphi_{\mathrm{PD}}$) from the SMI pattern. Despite an asymmetrical large dc component in the negative wing (due to an artifact—a tilt angle mismatch), the phase content is quite symmetrical and the extrema (maxima and minima) sequence is well defined. From the data of Figs. 2(a) and 2(b), we have extracted the angles of extrema points and computed phases $\Delta\varphi_{\mathrm{SMI}}$ and $\Delta\varphi_{\mathrm{PD}}$, whose difference is phase $\Delta\varphi$ given by Eq. (4). An example of measurement on a 154 μm glass slab is plotted in Fig. 3 as a function of rotation angle.

We can now fit the points in Fig. 3 by a theoretical curve, i.e., the right-hand side of Eq. (4). Doing so, we obtain a thickness $d = 157 \pm 3$ μm, in reasonable agreement to the measurement of slab thickness by a mechanical caliper, giving $d = 154 \pm 3$ μm (caliper accuracy depends on stiffness of material). A sample of a few measurements on glass slab samples of different thicknesses is reported in Table 1 to show the range of applicability of the method.

Results show that maximum error for a wide range of slab thickness is a few micrometers for thin slabs and around 10 μm for a thick, ~1 mm slab.

Going back to Eq. (2) with the result of thickness measurement, we can compute the index of refraction n. Using the above data, we can solve for n and find $n = 1.42$ for our glass slab. An estimate of accuracy for n obtained in this way from Eq. (2) can be obtained by taking the differential of the phase $\Delta\varphi_{\mathrm{PD}}$ in Eq. (2), so that

$$\Delta(\Delta\varphi_{\mathrm{PD}}) = 4\pi(d/\lambda)\Delta n \cos\theta + 4\pi(\Delta d/\lambda) n \cos\theta. \quad (5)$$

Putting numbers into Eq. (5), we get $\Delta n = \pm 0.04$, which is actually a large error, yet a value to start from to devise a better strategy if n has to be measured simultaneously to d.

Of course, all the above results hold under the assumption of a single-layer slab, whereas sometimes we have to deal with multilayer stacks. While we need a more complicated theory to treat the multilayer case, we have checked by numerical simulations that, if the refractive index in the layers has small variations, $\Delta n < 0.2$, we can apply the above results as a first-order approximation. For example, for a stack of two glass slabs, glued with a drop of polymer ~10 μm thick, we have measured $d = 335 \pm 10$ μm with respect to a true (mechanical) thickness of 342 μm, even though the refractive indices of the different layers varied by $\Delta n = 0.2$.

In conclusion, we have presented an SMI-based method of thickness measurement that is applicable to a wide range of slab thicknesses and is independent from the refractive index. Further study will deal with: analysis of the ultimate limits of the method, applicability to multilayer stacks, and extension to multiwavelength operation.

The authors thank Giuseppe Martini, who checked the validity of Eqs. (2) and (3) through an independent derivation. This work was supported in part by a MegaFrame EEC contract and in part by a Progetto Ricerca di Interesse Nazionale contract.

References

1. M. Debenham, G. Dew, and D. E. Putland, Opt. Acta **26**, 1487 (1979).
2. P. Tomlines, P. Wolliams, C. Hart, and A. Beaumont, Opt. Lett. **33**, 2272 (2008).
3. W. V. Sorin and D. F. Gray, IEEE Photonics Technol. Lett. **4**, 105 (1992).
4. G. Coppola, P. Ferraro, M. Lodice, and S. De Nicola, Appl. Opt. **42**, 3882 (2003).
5. P. de Groot, Appl. Opt. **39**, 2658 (2000).
6. K. Hibino, B. F. Oreb, P. S. Fairman, and J. Burke, Appl. Opt. **43**, 1241 (2004).
7. J. Heil, T. Bauer, S. Schmax, T. Sure, and J. Wesner, Appl. Opt. **46**, 5282 (2007).
8. S. Kim, J. Na, M. J. Kim, and B. H. Lee, Opt. Express **16**, 5516 (2008).
9. S. Donati, *Electro-Optical Instrumentation—Sensing and Measuring with Lasers* (Prentice Hall, 2004).
10. G. Giuliani, M. Norgia, S. Donati, and T. Bosch, J. Opt. A **4**, S283 (2002).
11. S. Donati, G. Giuliani, and S. Merlo, IEEE J. Quantum Electron. **31**, 113 (1995).